Laser-induced anisotropic wettability on azopolymeric micro-structures

Laser-induced anisotropic wettability on azopolymeric micro-structures

Cite as: Appl. Phys. Lett. **110**, 101603 (2017); https://doi.org/10.1063/1.4978260
Submitted: 21 December 2016 . Accepted: 24 February 2017 . Published Online: 07 March 2017

Federica Pirani, Angelo Angelini, Serena Ricciardi, Francesca Frascella, and Emiliano Descrovi

Laser-induced anisotropic wettability on azopolymeric micro-structures

Federica Pirani,[1,2] Angelo Angelini,[2] Serena Ricciardi,[2] Francesca Frascella,[2] and Emiliano Descrovi[2]
[1]*Centro per le Tecnologie Future Sostenibili, Istituto Italiano di Tecnologia, Corso Trento 21, 10129 Torino, Italy*
[2]*Dipartimento di Scienza Applicata e Tecnologia, Politecnico di Torino, C.so Duca degli Abruzzi 24, 10129 Torino, Italy*

(Received 21 December 2016; accepted 24 February 2017; published online 7 March 2017)

The light-induced deformation of a micro-textured photo-sensitive polymeric material is exploited for modifying the surface hydrophobicity along deterministic directions. Arrays of azopolymeric micro-pillars are fabricated over large area and irradiated with a green laser. Upon laser irradiation, the micro-pillars deform reversibly along a direction parallel to the laser polarization, resulting in elongated shapes with controllable eccentricity. Such a locally anisotropic topography induces a directional yet reversible change of hydrophobicity, as measured by contact angles varying within a range of 30°. *Published by AIP Publishing.* [http://dx.doi.org/10.1063/1.4978260]

The control of the wetting properties of micro-structured surfaces has attracted particular interest due to its applications in the fields of bio-nanotechnology, electronics, and diagnostics.[1] Since wettability is generally enhanced on rough surfaces, a variety of fabrication strategies, including soft lithography techniques[2] and laser micromachining,[3] have been employed in the past to obtain complex surface architectures. Within this framework, a big challenge is represented by the fabrication of structured surfaces able to undergo *in situ* variations in response to external stimuli, resulting in changes of wettability. The use of light-responsive materials can open interesting perspectives for triggering specific surface properties, such as anisotropic hydrophobic behavior,[4] upon proper light irradiation.[5]

Among light-sensitive materials, azopolymers have particular relevance. Azopolymers are polymeric compounds containing azobenzene groups that can undergo a reversible isomerization upon photon absorption.[6,7] Photoisomerization induces conformational changes both at a molecular and a macroscopic scale[8,9] resulting in light-induced variations of shape, phase, and wettability.[10] It is well known that the two azobenzene isomers exhibit different spatial arrangements and that the isomerization process can induce changes in the dipole moment.[11] The trans isomer has a small dipole moment and a low surface free energy resulting in a higher contact angle with water, while the cis form shows a lower contact angle due to its higher dipole moment and surface free energy.[12] This reversible trans to cis isomerization can be triggered by UV/visible irradiation, leading to a change in the surface hydrophobicity behavior. Ichimura *et al.*[13] and Radüge *et al.*[14] managed to induce light-driven wettability changes of a surface modified with a photoisomerizable azo-monolayer by exploiting a polarity change based on the molecular switching of the azobenzene groups included therein. Other approaches for obtaining photo-responsive surfaces with tunable wetting properties include Langmuir–Blodgett,[15] self-assembly,[16,17] and layer by layer methods.[18]

In addition to the surface chemical properties, surface topography is a relevant aspect affecting wettability.[19] In this work, we demonstrate that an *in situ* tunable hydrophobicity can be obtained upon light-induced deformation of arrays of azopolymeric micro-pillars. More specifically, micrometer-sized pillars are induced to elongate along the polarization direction of an incident laser radiation,[20] in such a way that an anisotropic change of wettability is produced according to the laser polarization direction. The proposed tuning of wettability based on light-induced topographic changes is partially reversible and can be easily applied to large area surfaces.

We use a Poly(Dispersed Red 1 methacrylate) (pDR1M) azopolymer formulation (Sigma Aldrich) (Fig. 1(a)). pDR1M is dissolved in tetrahydrofuran (anhydrous ≥99.9%, Sigma Aldrich) at a 2 wt. % concentration and then casted on a glass slide. The pDR1M film is patterned by soft-imprinting as an array of square micro-pillars. This technique involves the use of a Poly(dimethylsiloxane) (PDMS) mold to pattern the surface of the sample. The PDMS prepolymer (Dow Corning, Sylgard 184) is obtained by mixing the elastomer solution and the curing agent in a proper ratio (10:1 w/w). The mixture is poured onto a silicon master, whose surface has been patterned with the complementary structure to fabricate, and then left to cure in oven at 60 °C for 2 h. After curing, the PDMS is separated from the master and used as stamp for imprinting the pDR1M structure.

An amount up to 10 μl of pDR1M is casted on a clean glass slide and the PDMS stamp is kept in a conformal touch with the glass slide for 30 s at room temperature, under moderate pressure, leading the pDR1M polymer to fill the inner volumes of the mold (Fig. 1(b)). After the stamp is peeled off, the imprinted azopolymeric film is dried in oven (60 °C, 2 h) and an array of well- defined micro-pillars is finally obtained over an area of 2.5 mm × 2.5 mm. Scanning Electron Microscopy (SEM) and Atomic Force Microscopy (AFM) analyses reveal squared 3.5 μm × 3.5 μm × 1.1 μm pillars arranged in two dimensions, with 11 μm periodicity along each orthogonal direction (Fig. 1(c)).

The pDR1M structures undergo several cycles of laser-irradiation under a conventional optical microscope coupled to a laser source. The laser is a doubled frequency Nd:YAG cavity emitting a TEM_{00} beam at 532 nm wavelength, with an output power adjustable to a maximum of 250 mW. The

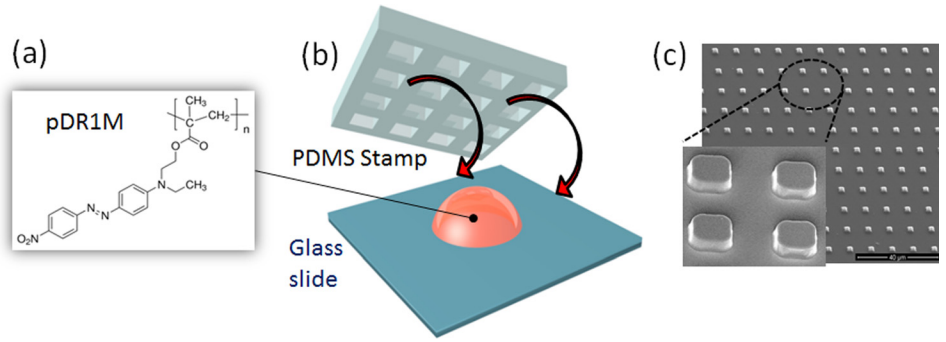

FIG. 1. (a) Chemical structure of Poly(Dispersed Red 1 methacrylate) and (b) sketch of the imprinting process by means of a PDMS stamp; (c) illustrative SEM image.

polarization is linear and can be rotated arbitrarily using a quarter-wavelength plate and a linear polarizer arrangement. The laser spot is expanded in such a way that a circular area of roughly 250 μm diameter can be homogeneously illuminated. During laser irradiation, a white-light wide-field imaging system (reflection) is employed to real-time monitor the deformation of the micro-pillars occurring along the polarization direction of the incident laser beam. An automatic pattern-recognition algorithm processes the collected images at a 1 Hz rate and performs image binarization and geometrical parameters extraction. A set of average roundness values over a sample area including roughly a hundred of micro-pillars is finally gathered. With this approach, the laser irradiation conditions can be real-time adjusted in such a way that elongated micro-pillars with a specific roundness value can be repeatedly obtained on different samples, as desired.

Once properly irradiated, contact angle measurements are performed over the illuminated area of the structure by employing a sessile drop method (Dataphysics OCA-20). A 0.5 μl water droplet is injected onto the sample surface through an automatic syringe. Each contact angle (CA) measurement is repeated by using three different water droplets, and then an average value and an associated square root mean value are calculated. All measurements presented here are performed under identical environmental conditions on four nominally identical samples, which have been laser processed according to the same irradiation protocol.

Figure 2 shows the average CA values as measured onto structured pDR1M samples featuring different pillar cross sections. More specifically, each data point corresponds to micro-pillars irradiated in a way to exhibit a specific mean roundness parameter ε, as estimated by the automatic image processing system. The mean roundness parameter ε is calculated as the ratio of the minor axis over the major axis, averaged over 120 micro-pillars. While a pDR1M flat surface is intrinsically hydrophobic because of its chemical structure ($CA = 85.2 \pm 2.5^\circ$), such a hydrophobicity is sensibly increased ($CA = 97.55 \pm 1.65^\circ$) when a textured pDR1M surface is considered, because of a largest effective surface area (data point (a) in Fig. 2). However, when micro-pillars are deformed along the incident polarization direction, with a roundness $\varepsilon = 0.71$, the contact angle is reduced to $CA = 79.52 \pm 0.90^\circ$ (data point (b) in Fig. 2). Such a CA change occurs anisotropically, along the elongation direction, as detailed in the following. For an 8 s overall irradiation time, micro-pillars further elongate to reach a mean roundness $\varepsilon = 0.51$. In this case, a corresponding average $CA = 72.250 \pm 0.9^\circ$ is observed (data point (c) in Fig. 2).

A rotation of the illumination polarization by 90° triggers a reconfiguration of the elliptical pillars resulting in a restoration of the initial shape.[20] Interestingly, the initial hydrophobicity is restored as well, as the contact angle increases back to value $CA = 89.41 \pm 1.5^\circ$ (data point (d) in Fig. 2).

However, we found this value as systematically slightly smaller than the initial one, probably because of some irreversible degradation effects occurring in the shape restoring process. For each fresh sample, we observed that up to two irradiation cycles can be performed with a good reversibility in morphology and wettability characteristics. The error bar for the CA measurement at point (d) in Fig. 2 is taking into account variation in the micropillar shape restoring process over two irradiation cycles. For longer irradiation times (larger than 8 s) at a fixed polarization direction, pillars become irreversibly elongated, with mean roundness values $\varepsilon < 0.38$, eventually merging together to form twisty linear gratings. As a smaller amount of air is trapped underneath the water droplet, a further decrease of the contact angle is observed, down to $CA = 64 \pm 1.3^\circ$ (data point (e) in Fig. 2).

The contact angle measurements presented are taken along a direction parallel to the elongation of micro-pillars. In fact, as the surface structure exhibits an anisotropic

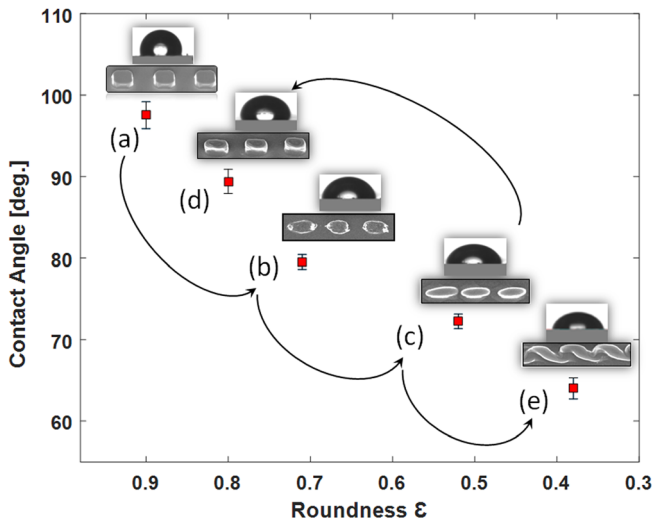

FIG. 2. Mean contact angle as a function of the micro-pillar roundness. Data points correspond to (a) as-fabricated sample; (b) first step of elongation (3 s irradiation); (c) second step of elongation (8 s irradiation); (d) recovery of the initial shape; and (e) irreversible elongation. In the insets, representative water droplet images and SEM images corresponding to each micro-pillar arrangement are shown.

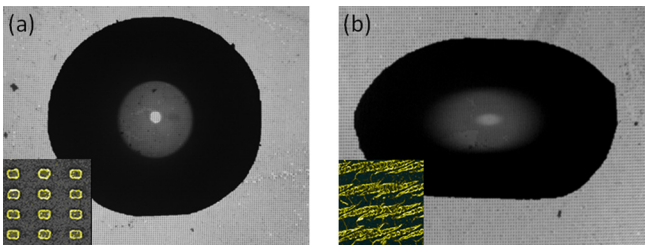

FIG. 3. Wide-field reflection images of water droplets deposited onto pDR1M micropillars taken from above; (a) as-fabricated sample with squared pillars; (b) strongly elongated pillars along the horizontal direction. Insets: illustrative SEM images of the corresponding surface structures.

topography, the water droplet arrangement on the sample is anisotropic as well.

In Figure 3 two water droplets (0.5 μl) left onto either an as-fabricated or an irradiated sample are optically imaged from above.

While the two-dimensional symmetry of the as-fabricated micro-pillar array induces the droplet to arrange isotropically (Fig. 3(a)), the symmetry breaking due to laser irradiation results in a water droplet significantly spreads along a direction parallel to the micro-pillar elongation (Fig. 3(b)).

In order to understand the experimental observation presented above, an AFM analysis is performed. Here we consider the topography of three illustrative cases, comprising (1) as-fabricated, (2) slightly elongated, and (3) strongly elongated pillars. From AFM maps shown in Figs. 4(a)–4(c), topographic cross-sections along the two orthogonal directions of the square lattices are extracted. In Figures 4(d)–4(f), V-cross-sections (parallel to the polarization direction) reveal that the inter-pillar distance is significantly decreasing from $d = 7.5\ \mu m$ (as-fabricated) to $d_1 = 2.3\ \mu m$ (slight elongation), down to $d_2 = 1.2\ \mu m$ (strong elongation).

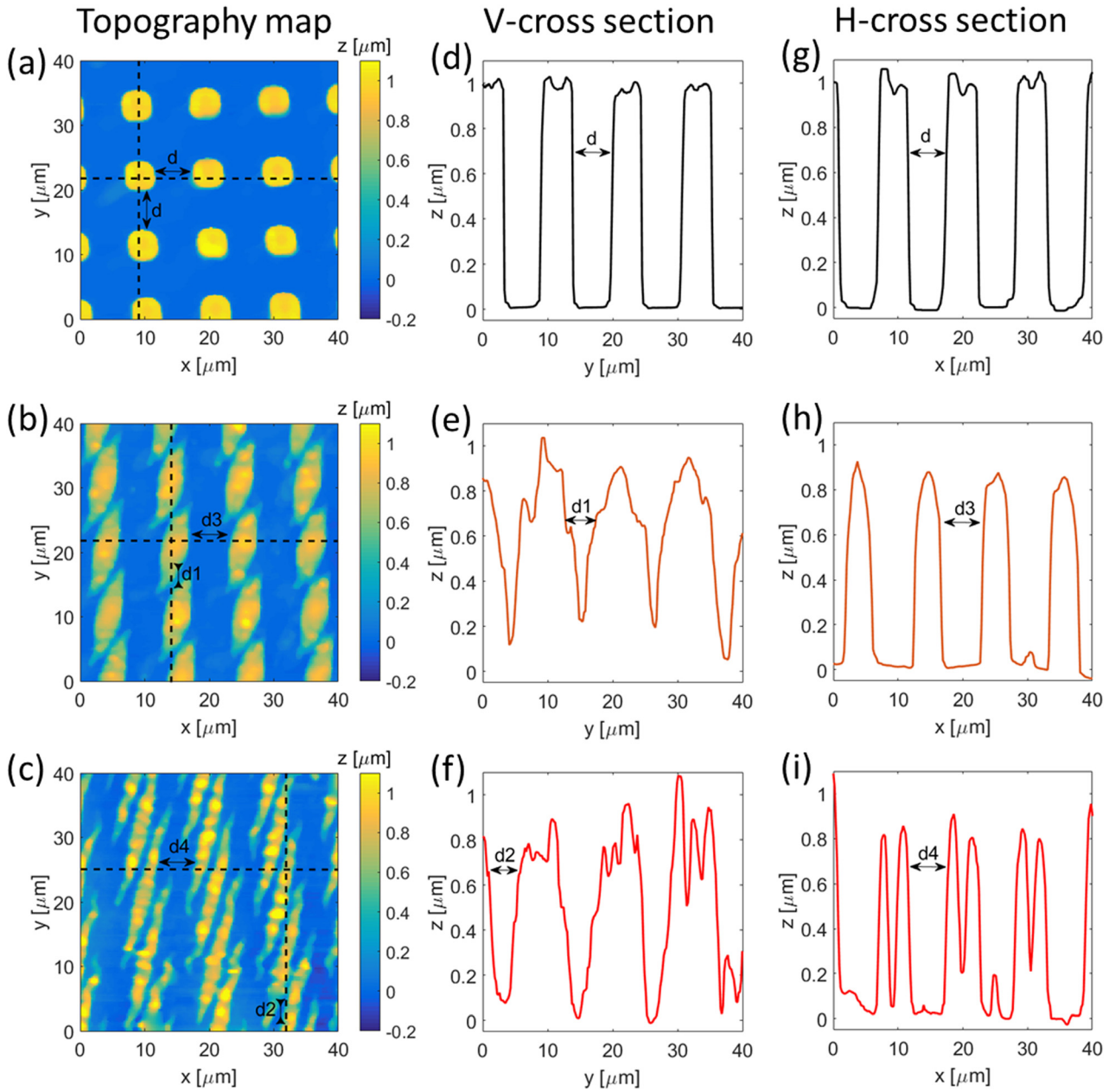

FIG. 4. AFM maps and topographic cross sections of pDR1M textured surfaces: (a), (d), (g) as-fabricated; (b), (e), (h) irradiated for 8 s; and (c), (f), (i) irradiated for 12 s.

Furthermore, perpendicularly to the polarization direction, the inter-pillar distance is maintained at a rather similar value to the as-fabricated sample ($d_3 = d_4 \sim 7\ \mu m$), as shown by the H-cross sections presented in Figs. 4(g)–4(i).

As it is well-known that texture-induced wettability depends on the amount of air trapped within the surface corrugations, below the water droplet,[21] we explain the observed anisotropic decrease of hydrophobicity as an anisotropic distribution of such trapped air volumes. It is worth to note that the pillar height is observed as almost constant ($\sim 1\ \mu m$) regardless of the elongation state of the pillars, with just a slightly decrease of less than 300 nm in the strong elongation state. This observation supports a change of hydrophobicity as mainly related to the modified pillar cross section rather than a drastic decrease of the pillar height.

Thanks to a precise spatio-temporal control of the light-induced deformation of an azopolymeric microstructure, we are able to alter its surface wettability along preferential directions. Such an anisotropy is obtained by making the pillars elongating according to the polarization direction of an illumination laser. In this work we managed to vary the contact angle of a water droplet on the structure by more than 30°. This process can be partially reversed provided that the pillar elongation is kept within a roundness larger than about 0.5. However, other azopolymeric compounds can be used to improve reversibility of deformation.

The ability to tune and recover the surface hydrophobicity along specific directions may open up future promising applications, including functional biomimetic surfaces and tunable smart material architectures for cell cultures, wherein azo-compounds can provide additional chemical functionalities.[22,23]

This research has received funding from the Italian Flagship Project NANOMAX (Progetto Bandiera MIUR PNR 2011–2013) and the Italian FIRB 2011 NEWTON (RBAP11BYNP). Mr. Mauro Raimondo (DISAT, Politecnico di Torino) is greatly acknowledged for technical assistance.

[1]M. A. C. Stuart, W. T. S. Huck, J. Genzer, M. Müller, C. Ober, M. Stamm, G. B. Sukhorukov, I. Szleifer, V. V. Tsukruk, M. Urban, F. Winnik, S. Zauscher, I. Luzinov, and S. Minko, Nat. Mater. **9**, 101 (2010).
[2]B. Liu, Y. He, Y. Fan, and X. Wang, Macromol. Rapid Commun. **27**, 1859 (2006).
[3]G. Caputo, B. Cortese, C. Nobile, M. Salerno, R. Cingolani, G. Gigli, P. D. Cozzoli, and A. Athanassiou, Adv. Funct. Mater. **19**, 1149 (2009).
[4]S. Lee, H. S. Kang, A. Ambrosio, J. K. Park, and L. Marrucci, ACS Appl. Mater. Interfaces **7**, 8209 (2015).
[5]A. Athanassiou, M. Varda, E. Mele, M. I. Lygeraki, D. Pisignano, M. Farsari, C. Fotakis, R. Cingolani, and S. H. Anastasiadis, Appl. Phys. A: Mater. Sci. Process. **83**, 351 (2006).
[6]C. J. Barrett, J. Mamiya, K. G. Yager, and T. Ikeda, Soft Matter **3**, 1249 (2007).
[7]A. Priimagi and A. Shevchenko, J. Polym. Sci., Part B: Polym. Phys. **52**, 163 (2014).
[8]G. S. Kumar and D. C. Neckers, Chem. Rev. **89**, 1915 (1989).
[9]A. Natansohn and P. Rochon, Chem. Rev. **102**, 4139 (2002).
[10]M. M. Russew and S. Hecht, Adv. Mater. **22**, 3348 (2010).
[11]J. Groten, C. Bunte, and J. Rühe, Langmuir **28**, 15038 (2012).
[12]B. Xin and J. Hao, Chem. Soc. Rev. **39**, 769 (2010).
[13]K. Ichimura, S.-K. Oh, and M. Nakagawa, Science **288**, 1624 (2000).
[14]C. Radüge, G. Papastavrou, D. G. Kurth, and H. Motschmann, Eur. Phys. J. E **10**, 103 (2003).
[15]C. L. Feng, Y. J. Zhang, J. Jin, Y. L. Song, L. Y. Xie, G. R. Qu, L. Jiang, and D. B. Zhu, Langmuir **17**, 4593 (2001).
[16]W. Jiang, G. Wang, Y. He, X. Wang, Y. An, Y. Song, and L. Jiang, Chem. Commun. **3550** (2005).
[17]N. Delorme, J.-F. Bardeau, A. Bulou, and F. Poncin-Epaillard, Langmuir **21**, 12278 (2005).
[18]M. Y. Paik, S. Krishnan, F. You, X. Li, A. Hexemer, Y. Ando, S. H. Kang, D. A. Fischer, E. J. Kramer, and C. K. Ober, Langmuir **23**, 5110 (2007).
[19]T. Sun, G. Wang, L. Feng, B. Liu, Y. Ma, L. Jiang, and D. Zhu, Angew. Chem., Int. Ed. **43**, 357 (2004).
[20]F. Pirani, A. Angelini, F. Frascella, R. Rizzo, S. Ricciardi, and E. Descrovi, Sci. Rep. **6**, 31702 (2016).
[21]J. T. Yang, Z. H. Yang, C. Y. Chen, and D. J. Yao, Langmuir **24**, 9889 (2008).
[22]S. Piotto, S. Concilio, L. Sessa, P. Iannelli, A. Porta, E. C. Calabrese, M. R. Galdi, and L. Incarnato, Polym. Compos. **34**, 1489 (2013).
[23]S. Piotto, S. Concilio, L. Sessa, P. Iannelli, A. Porta, E. C. Calabrese, A. Zanfardino, M. Varcamonti, and P. Iannelli, Eur. J. Med. Chem. **68**, 178 (2013).